

Highly Hydrothermally Stable Microporous Silica Membranes for Hydrogen Separation

Qi Wei,[†] Fei Wang,[†] Zuo-Ren Nie,^{*,†} Chun-Lin Song,[‡] Yan-Li Wang,[†] and Qun-Yan Li[†]

College of Materials Science & Engineering, Beijing University of Technology, 100 Pingleyuan, Chaoyang District, Beijing 100022, People's Republic of China, and Inorganic Membranes, Faculty of Science and Technology & MESA⁺ Institute for Nanotechnology, University of Twente, P.O. Box 217, 7500 AE Enschede, The Netherlands

Received: December 8, 2007; Revised Manuscript Received: May 20, 2008

Fluorocarbon-modified silica membranes were deposited on γ -Al₂O₃/ α -Al₂O₃ supports by the sol–gel technique for hydrogen separation. The hydrophobic property, pore structure, gas transport and separation performance, and hydrothermal stability of the modified membranes were investigated. It is observed that the water contact angle increases from $27.2 \pm 1.5^\circ$ for the pure silica membranes to $115.0 \pm 1.2^\circ$ for the modified ones with a (trifluoropropyl)triethoxysilane (TFPTES)/tetraethyl orthosilicate (TEOS) molar ratio of 0.6. The modified membranes preserve a microporous structure with a micropore volume of 0.14 cm³/g and a pore size of ~ 0.5 nm. A single gas permeation of H₂ and CO₂ through the modified membranes presents small positive apparent thermal activation energies, indicating a dominant microporous membrane transport. At 200 °C, a single H₂ permeance of 3.1×10^{-6} mol m⁻² s⁻¹ Pa⁻¹ and a H₂/CO₂ permselectivity of 15.2 were obtained after proper correction for the support resistance and the contribution from the defects. In the gas mixture measurement, the H₂ permeance and the H₂/CO₂ separation factor almost remain constant at 200 °C with a water vapor pressure of 1.2×10^4 Pa for at least 220 h, indicating that the modified membranes are hydrothermally stable, benefiting from the integrity of the microporous structure due to the fluorocarbon modification.

Introduction

As a clean fuel, hydrogen has drawn much attention in recent years because of the rapid consumption of petroleum oil reserves and the serious environmental pollution caused by the excess utilization of fossil fuels.¹ Currently, ~ 41 million metric tons/yr of H₂ is produced worldwide. As high as 80% of H₂ is produced from natural gas by steam re-forming, partial oxidation, and autothermal re-forming.² The continuous removal of H₂ from the reaction mixture through the H₂-selective membranes provides a number of advantages: high conversion, high selectivity, low operating temperatures, and reduced catalyst requirements, etc.^{3–5} A sol–gel-derived microporous silica membrane ($\phi_p < 2$ nm) is one of the promising candidates for hydrogen separation because of its ease of preparation, pore size at the gas molecule level, and high porosity, etc.^{6–10} However, the hydrothermal stability is a key issue for silica membranes used under the conditions of high temperatures and the presence of water vapor.^{11–15} A reduced gas flux (as much as 50% or greater) and a decreased selectivity were reported within the first few hours after the silica membranes were exposed to water vapor.^{13,16–18} This decline is generally caused by the deterioration of pore structures resulting from the attack of H₂O molecules. It is believed that silanols (hydroxyl groups) on the pore surface are sensitive to the H₂O molecules; therefore, replacing the silanols with some hydrophobic groups is an alternative strategy to reduce water adsorption and maintain gas separation properties.¹⁸ A large number of functional groups have been used to improve the hydrophobic property of aerogel and silica glass,^{19–23} but scarce studies on hydrophobic silica membranes have been reported. Renate de Vos et al. are the

first pioneers who prepared the hydrophobic methyl-modified silica membranes by adapting the synthesis of the sol.¹¹ It is well-known that fluorocarbon groups are highly hydrophobic, but few investigations have focused on the silica membranes modified by fluorocarbon groups except for several reports on the fluorinated silica monolith or gels.^{24,25} In the present paper, the silica membranes modified with fluorocarbon groups were prepared by the sol–gel method. Their hydrophobic property, pore structure, gas transport and separation performance, and hydrothermal stability were studied.

Experimental Methods

Silica Membrane Preparation. Silica sols were prepared by the acid-catalyzed hydrolysis and condensation of TEOS (Acros) in an EtOH (Acros) medium as described in the literature.⁶ The fluorocarbon-modified membranes were obtained by the cohydrolysis and condensation of TEOS and TFPTES (Acros). A mixture of water and HNO₃ was added slowly to a solution of EtOH and TEOS with a TEOS/EtOH/H₂O/HNO₃ molar ratio of 1/3.8/6.4/0.085, which was mixed homogeneously in an ice bath previously. Then the mixture was heated to 60 °C and refluxed for 2.5 h to obtain solution A. Another solution, B, was prepared by mixing TFPTES with EtOH according to a TFPTES/EtOH molar ratio of 0.2–0.6/3.8. Solution B was then added to solution A and reacted for 30 min at 60 °C during stirring to get a final sol with a TEOS/TFPTES/EtOH/H₂O/HNO₃ molar ratio of 1/0.2–0.6/7.6/6.4/0.085. The final sol was diluted 19 times with EtOH to obtain a dipping sol. The supported silica membranes were prepared on the top of γ -Al₂O₃ membranes supported by α -Al₂O₃ ceramic by dip-coating in a clean room (grade 100). The dip-coating process was carefully controlled by a dip-coater to contact the sol and move horizontally. After coating, the samples were dried and then calcined at 400 °C for 5 h with a heating and cooling rate of 1

* To whom correspondence should be addressed. E-mail: znie@bjut.edu.cn. Phone/fax: 86-10- 67391536.

[†] Beijing University of Technology.

[‡] University of Twente.

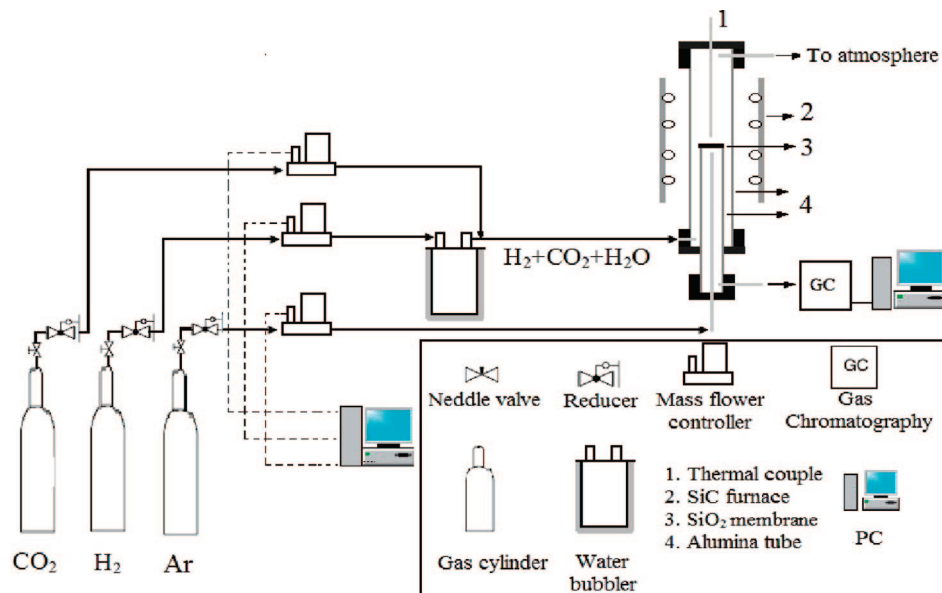


Figure 1. Diagram of a setup for gas permeation and separation.

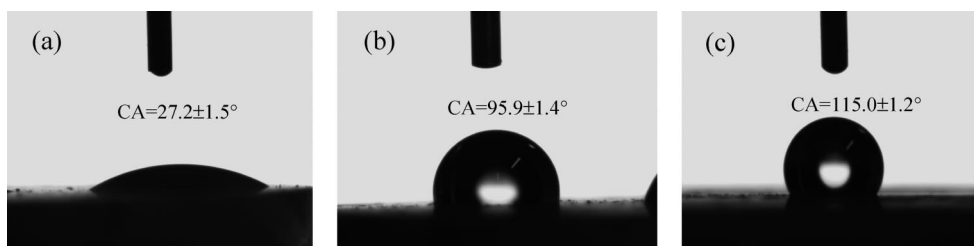


Figure 2. Shape of a water droplet on the surface of SiO₂ (a), (0.2TFPTES)SiO₂ (b), and (0.6TFPTES)SiO₂ (c) membranes.

°C/min in a N₂ atmosphere. The dip-coating and calcinations were repeated twice to reduce the surface defects. The rest of the sol was poured into a Petri dish and dried at room temperature; after gelation, the gel was calcined under the conditions for the supported membranes and used to conduct NMR and N₂ adsorption measurements. In this paper, SiO₂, (0.2 TFPTES)SiO₂, and (0.6 TFPTES)SiO₂ denote the pure silica membranes and the modified ones with a TFPTES/TEOS molar ratio of 0.2 and 0.6, respectively.

Membrane Characterization. The water contact angle was measured by a Dataphysics OCA20 video-based contact angle system at room temperature. A water droplet of ~1 μ L was dropped carefully onto the membrane surface. Infrared spectra were measured by a Nicolet 5700 FT-IR spectrophotometer with a resolution of 4 cm⁻¹ and a scan number of 32. Solid-state ²⁹Si MAS NMR spectra were recorded by a Bruker AV300 spectrometer according to the following measurement conditions: 5 mm MAS probe, 59.62 MHz resonance frequency, $\pi/2$ pulse, 6.0 μ s pulse width, 5 kHz magic-angle spin, 600 s delay time, and 200 scans. Chemical shifts were referenced to TMS at 0 ppm. Thermal analysis experiments were conducted on a Netzsch STA 449C thermal analyzer with a heating rate of 10 °C/min to 650 °C under a 30 mL/min N₂ flow. Nitrogen adsorption measurements were carried out at 77 K on a Micromeritics ASAP 2020 M volumetric adsorption analyzer. Before the measurements, the samples were outgassed under vacuum at 300 °C for 72 h. The total pore volume was calculated at the saturated pressure. The micropore volume was determined from the *t*-plot, and the micropore size distribution was calculated according to the SF-modified HK method using the physical parameters suitable for microporous silica materials.²⁶ It is worth noting that the HK method is based on a fundamental

statistical analysis of a fluid confined to a slit pore (e.g., applicable to carbon molecular sieves and active carbons) and describes a semiempirical calculation of the effective pore size distributions from nitrogen adsorption isotherms in the microporous materials.²⁷ Saito and Foley extended the HK method for a cylindrical pore geometry (e.g., applicable to zeolite and silica).²⁸

Gas Permeation, Separation, and Hydrothermal Stability.

The single gas permeance of the supported membranes was measured with a dead-end setup.²⁹ The membrane was sealed by a fluorinated latex O-ring on one side of an alumina tube, and the microporous SiO₂ layer was exposed to the feed gas. The gas pressure was maintained at 1 atm at the permeate side and 2 atm at the feed side. The gas flux at the permeate side was measured with a soap-bubble meter.

The hydrothermal stability was represented by the H₂ permeance and the H₂/CO₂ separation factor under a humid gas mixture atmosphere for a long term, which were obtained with a homemade setup (Figure 1). The experimental routes are described as follows: H₂ passed through a water bubbler and then was mixed with CO₂ at the outlet of the water bubbler. The feed gas mixture of H₂, CO₂, and H₂O entered the outer alumina tube and permeated through the membranes to the permeate side. The pressure at both the feed and permeate sides was preserved at 1 atm. The partial pressure of H₂ and CO₂ at the permeate side depends on their concentration in the gas mixture, which could be analyzed by GC with the help of the carrier gas, i.e., Ar. The permeance of H₂ and CO₂ was calculated on the basis of the partial pressure at both the feed and permeate sides and the gas flux at the permeate side. The partial pressure of water vapor was estimated from the saturated vapor pressure of the distilled water at an experimental

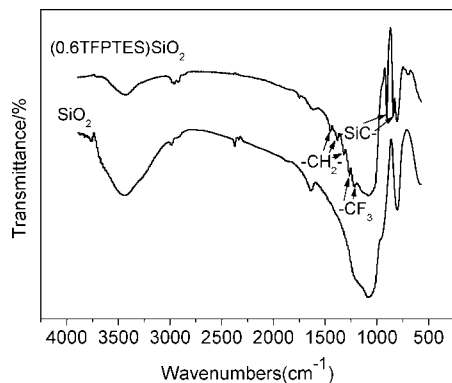


Figure 3. FT-IR spectra of the pure and the modified silica membranes.

temperature and could be easily changed by adjusting the temperature of distilled water (in this work, the pressure of water vapor is 1.2×10^4 Pa). The separation factor (α) of a gas mixture of H_2 and CO_2 is calculated from the gas concentration (C_{feed} , C_{permeate}) at the feed and permeate sides according to the following equation:

$$\alpha = \frac{C_{H_2, \text{permeate}}}{C_{CO_2, \text{permeate}}} \frac{C_{CO_2, \text{feed}}}{C_{H_2, \text{feed}}} \quad (1)$$

Results and Discussion

Figure 2 shows the shape of a water droplet on the surface of the pure and the modified silica membranes. The water CA increases from $27.2 \pm 1.5^\circ$ for the pure silica membrane to $95.9 \pm 1.4^\circ$ for the (0.2TFPTES)SiO₂ membrane and $115.0 \pm 1.2^\circ$ for the (0.6TFPTES)SiO₂ membrane, indicating that the hydrophobic property has been dramatically enhanced due to the surface modification with fluorocarbon groups. This improvement could benefit from the replacement of silanols by hydrophobic groups. In this section, the modified membrane is referred to as (0.6TFPTES)SiO₂ if not otherwise stated.

The successful modification by the fluorocarbon groups is further confirmed by FT-IR spectra, shown in Figure 3. The absorption peaks over the range from 1450 to 1210 cm^{-1} and from 903 to 838 cm^{-1} indicate the presence of the fluorocarbon groups in the modified samples.^{24,30} The peaks at 1449, 1379, and 1319 cm^{-1} can be attributed to the bending vibration, the wagging vibration, and the twisting vibration of $-\text{CH}_2-$, respectively. The peaks at 1266 and 1215 cm^{-1} can be assigned to the asymmetrical stretching vibration and the symmetrical stretching vibration of $-\text{CF}_3$, respectively. The absorption peaks of Si-C correspond to the bands around 904 and 840 cm^{-1} . However, the above-mentioned absorption bands are not observed in the pure silica membranes. It is very crucial to note that the IR signal due to the physisorbed water ($\sim 3442 \text{ cm}^{-1}$) significantly decreases in the modified sample, which further demonstrates the enhancement of the hydrophobic property.

The amount of fluorocarbon groups and surface silanols in the membranes was quantitatively determined by solid-state ^{29}Si MAS NMR. The spectra, fitted by the Gaussian approach, are shown in Figure 4. The resonances at the chemical shifts of -112 , -100 , and -90 ppm can be assigned to Q^4 , Q^3 , and Q^2 silicon atoms, respectively.^{31,32} Two additional resonances due to the fluorocarbon groups, which are linked to silicon atoms, T^3 at -66 ppm and T^2 at -53 ppm, can also be observed in the modified materials.^{31–33} Integrating the Q^m and T^n resonances will give the relative percentage of each species in the matrixes,

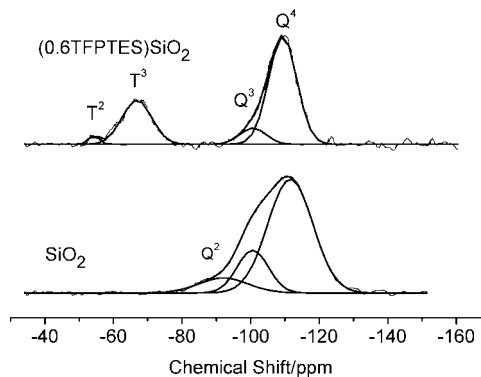


Figure 4. Solid-state ^{29}Si MAS NMR spectra of the pure and the modified silica membranes.

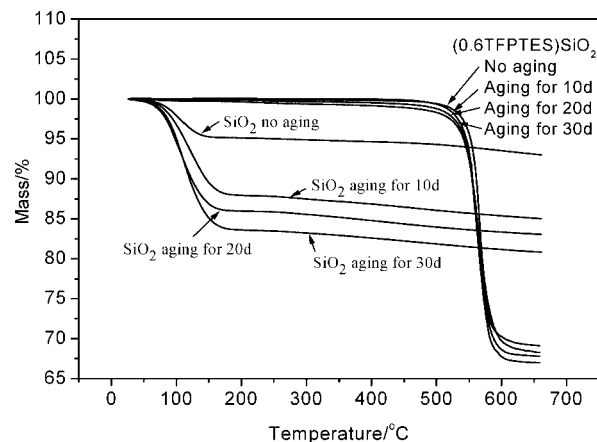


Figure 5. Thermogravimetric curves of the pure and the modified silica membranes exposed to a humid atmosphere for different times.

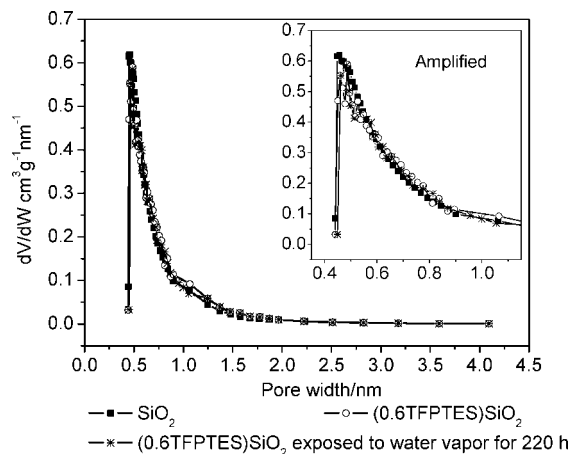


Figure 6. Pore size distribution of the pure and the modified silica membranes.

and the results are listed in Table 1. The results show that fluorocarbon groups have been incorporated into the modified silica membranes and the amount reaches 3.6 mmol/g. The concentration of surface silanols sharply decreases from 10.3 mmol/g for the pure silica membranes to 2.7 mmol/g for the modified ones. The presence of hydrophobic fluorocarbon groups and the decrease of hydrophilic silanols are responsible for the enhancement of the hydrophobic property of the modified membranes. Furthermore, the absence of the Q^2 signal in the sample (0.6TFPTES)SiO₂ indicates a high condensation degree, which makes the number of the residual surface silanols as small as possible.³⁴

TABLE 1: Solid-State ²⁹Si MAS NMR Results of the Pure and the Modified Silica Membranes

membrane	[Q ⁴] (mol %)	[Q ³] (mol %)	[Q ²] (mol %)	[T ³] (mol %)	[T ²] (mol %)	[OH] (mmol/g)	[C ₂ H ₄ CF ₃] (mmol/g)
SiO ₂	55.0	22.2	22.8			10.3	
(0.6TFPTES)SiO ₂	49.4	17.6		25.8	7.2	2.7	3.6

TABLE 2: Single Gas Permeance ($\times 10^{-7}$ mol m⁻² s⁻¹ Pa⁻¹) through the Supported Modified Silica Membranes (f^{tot}) and the γ -Al₂O₃/α-Al₂O₃ Supports (f^{sup})

gas	50 °C		100 °C		150 °C		200 °C		250 °C	
	f^{tot}	f^{sup}	f^{tot}	f^{sup}	f^{tot}	f^{sup}	f^{tot}	f^{sup}	f^{tot}	f^{sup}
H ₂	14.2	35.4	14.8	33.6	15.5	30.6	16.3	28.5	16.9	28.1
CO ₂	2.35	9.0	2.35	7.8	2.36	7.0	2.38	6.9	2.39	6.4
SF ₆	0.84	5.1	0.81	4.4	0.77	4.0	0.72	3.8	0.7	3.2

Thermogravimetric analysis results on the pure and the modified membranes are shown in Figure 5. The samples were pretreated at a temperature of 40 °C for different times in a closed atmosphere with a relative humidity of 75–80%. In Figure 5, the weight loss at temperatures lower than 200 °C is attributed to the evaporation of the physisorbed water. A weight loss due to the physisorbed water occurs for the pure silica membranes, for samples with no aging (4.9%) or aging for 10 d (12.1%), 20 d (14.0%), and 30 d (16.4%). However, no weight loss below 200 °C was observed for the modified ones, suggesting that water adsorption from the environment hardly takes place in these materials.³⁵ Generally, the amount of the adsorbed water depends on a lot of parameters, such as the porosity and the surface properties. Since the modified membranes have almost the same pore structure as that of the pure ones (Figure 6), the hydrophobic surface on the modified membranes, owing to the fluorocarbon groups, is reasonable to reduce the water adsorption to a large extent. Thus, the preservation of the microporous structure of the modified membranes can be expected when they are used under a humid atmosphere. An obvious weight loss observed at temperatures as high as 500 °C for the modified membranes may be due to the thermal decomposition of organic groups, indicating a high thermal stability of the modified membranes.

The pore structure of the samples was analyzed by N₂ adsorption. The total pore volume is 0.22 and 0.19 cm³/g and the surface area is 444.2 and 408.8 m²/g for the pure and the modified materials, respectively. As calculated from *t*-plots of the results, more than 76.1% and 71.1% of the pore volume of the pure and the modified materials, respectively, is associated with micropores, confirming that the samples have a microporous structure. The micropore size distributions calculated with the SF-modified HK method indicate that both the pure and the modified silica membranes have a narrow pore size centered at ~0.5 nm (Figure 6). Such a pore size is of particular significance for the applications of gas separation.

The results of the single gas permeance of H₂, CO₂, and SF₆ through the supported modified silica membranes and the γ -Al₂O₃/α-Al₂O₃ supports under temperatures ranging from 50 to 250 °C are shown in Table 2. It can be seen that the f^{tot} of H₂ and CO₂ increases slightly with increasing temperatures and the permselectivity of H₂/CO₂ varies from 6 to 7, showing that the transport in the supported modified membranes is controlled by micropore diffusion. f^{sup} of all the studied gases decreases slightly with increasing temperatures, displaying a temperature dependence of Knudsen diffusion. As claimed by Verweij et al.,³⁶ the flux and the separation factor of many high-flux supported membranes are often affected by the support resistance. Compared to f^{tot} , f^{sup} is not high enough, and thus, the influence from the support cannot be neglected. f^{top} of the

TABLE 3: Single Gas Permeance ($\times 10^{-7}$ mol m⁻² s⁻¹ Pa⁻¹) of the Modified Silica Membranes after Correction for the Support Resistance

gas	50 °C	100 °C	150 °C	200 °C	250 °C
H ₂	23.7	26.4	31.4	38.1	42.4
CO ₂	3.18	3.36	3.56	3.63	3.81
SF ₆	1.0	0.99	0.95	0.89	0.90

membrane layer can be obtained from f^{tot} and f^{sup} by the following relationship:

$$\frac{1}{f^{\text{tot}}} = \frac{1}{f^{\text{sup}}} + \frac{1}{f^{\text{top}}} \quad (2)$$

Subsequently, all the gas permeances were corrected to take the support resistance into account, and the results are shown in Table 3.

SF₆ is not able to permeate through the micropores of the modified membranes (most of them are less than 0.5 nm in diameter) in terms of its kinetics diameter ($d_k = 0.55$ nm), so it can be considered as a nonpermeable gas for the modified membranes. However, a SF₆ permeance on the order of 10⁻⁸ mol m⁻² s⁻¹ Pa⁻¹, decreasing with increasing temperatures, was observed in the modified membranes (Table 2). This phenomenon indicates that the defects are likely to be present on the top silica membranes. In this paper, SF₆ transport through the defects is assumed to comply with Knudsen diffusion. According to Knudsen diffusion, the ideal separation factor (permselectivity, α^*) of two gases equals the square root of the ratio of the gas masses, $\alpha^* = \sqrt{(M_2/M_1)}$, with $M_2 > M_1$; therefore, $\alpha^*(\text{H}_2/\text{SF}_6) = 8.54$ and $\alpha^*(\text{CO}_2/\text{SF}_6) = 1.82$. The contribution of Knudsen permeance of H₂ and CO₂ through the defects can be derived from that of SF₆, and then the real microporous permeance ($f^{\text{top-Kn}}$) can be obtained by subtracting the Knudsen contribution from the total permeance and correcting for the support resistance. The results are shown in Figure 7. The apparent thermal activation energies, $-u^{\text{tot}}$, of the permeance can be calculated. According to the model for microporous membrane transport,³⁶ the assumption that gas molecules transport in the micropores by hopping from a sorption site to another adjacent vacant one in a Langmuir lattice, was made. Molecules in the micropores can be considered as trapped in a potential well with a depth roughly equal to the standard partial molar enthalpy of sorption (Δh°). This means that the hopping energy, u^h , has a magnitude similar to $\sim \Delta h^\circ$, which in turn results in a fairly weak temperature dependence of permeance. The rather small apparent thermal activation energies, $-u^{\text{tot}}$, in the present work indicate a weak temperature dependence, which is in good agreement with the above model. Furthermore, the positive apparent thermal activation energies of H₂ and CO₂ are also an indication of the dominant microporous membrane transport.

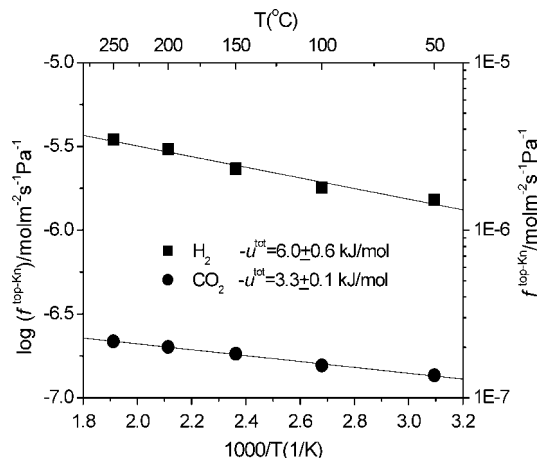


Figure 7. Arrhenius plot of $f^{\text{top-Kn}}$ through the modified silica membranes.

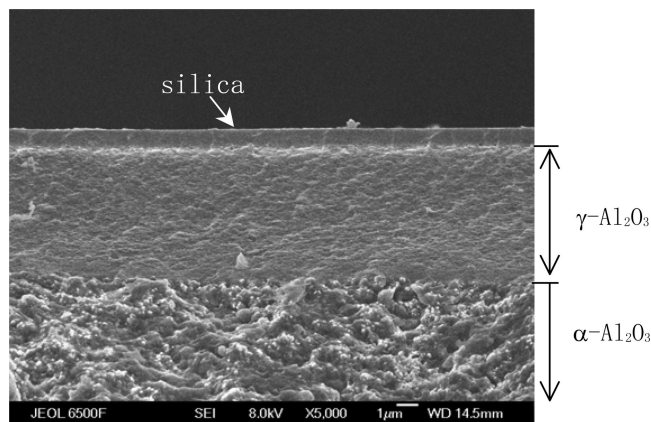


Figure 8. SEM photo of the cross-section of the modified silica membranes exposed to a humid atmosphere for 220 h.

It has been reported that the supported mesoporous $\gamma\text{-Al}_2\text{O}_3$ membranes deteriorate in a steam-containing environment at high temperatures, including the delamination of the $\gamma\text{-Al}_2\text{O}_3$ membranes from the $\alpha\text{-Al}_2\text{O}_3$ supports or a large change in pore size under the hydrothermal conditions.³⁷ In this work, the deterioration of the $\gamma\text{-Al}_2\text{O}_3$ layer was not observed, probably owing to the relatively low operating temperatures and a low steam concentration. Additionally, it was reported that the phase transformation of $\gamma\text{-Al}_2\text{O}_3$, which leads to a considerable pore change, does not occur at temperatures lower than 200 °C.³⁸ Figure 8 shows the cross-section of the modified membrane after exposure to a humid atmosphere with a water vapor pressure of 1.2×10^4 Pa at 200 °C for 220 h. It can be seen that the $\gamma\text{-Al}_2\text{O}_3$ layer adheres tightly to both sides, rather than peels from the modified silica layer and the $\alpha\text{-Al}_2\text{O}_3$ support.

The gas transport and separation behavior was investigated at 200 °C and in an atmosphere containing water vapor for a long term to reveal the hydrothermal stability of the modified silica membranes, and the result is shown in Figure 9. The overall H_2 permeance and H_2/CO_2 separation factor almost remain constant even after exposure to water vapor for 220 h, presenting a significant contrast to the pure silica membranes whose permeance decreases sharply in the first several hours due to the deterioration of the pore structure in the humid atmosphere. This observation also suggests that the modified membranes are highly hydrothermally stable under the studied conditions. In combination with the results in Figure 6 where the pore structure of the modified membranes exposed to steam

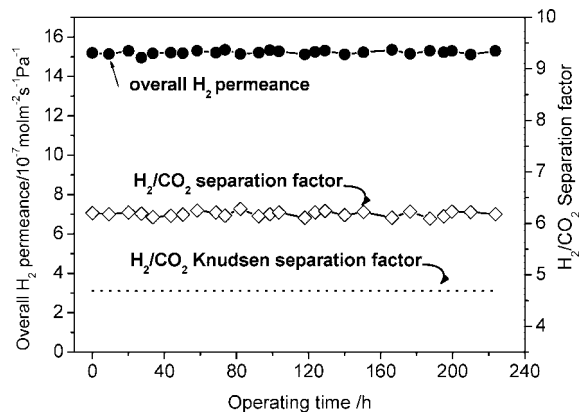


Figure 9. Time dependence of the H_2 permeance and H_2/CO_2 separation factor on the modified membranes under hydrothermal conditions.

for 220 h remains almost intact, it is believed that the integrity of the pore structure is responsible for the hydrothermal stability. It has been reported that the hydrophilic nature of the pure silica membranes leads to the expansion of pore space and a reduction of pore connectivity.³⁹ However, for the modified membranes in this work, the pore size can be stabilized within the micropore range because the hydrophobic surface significantly reduces the water adsorption and then prevents the expansion of the pore size.

Conclusion

Hydrophobic silica membranes with a water contact angle of $115.0 \pm 1.2^\circ$ are obtained by the cohydrolysis and condensation reaction of tetraethyl orthosilicate and (trifluoropropyl)triethoxysilane. The modified silica membranes preserve a microporous structure with a narrow pore size distribution centered at 0.5 nm, and such a microporous structure can be retained after exposure to water vapor for 220 h. Single gas permeance through the modified membranes has positive apparent thermal activation energies, indicating a dominant microporous membrane transport. The modified membranes are hydrothermally stable, and the H_2 permeance and H_2/CO_2 separation factor at 200 °C remain almost constant for at least 220 h under hydrothermal conditions. The hydrothermal stability of the membranes is due to the integrity of the microporous structure benefiting from the fluorocarbon groups on the surface.

Acknowledgment. This project is financially supported by the National Natural Science Foundation of China (Grant Nos. 50502002 and 50525413) and Scientific Research Common Program of the Beijing Municipal Commission of Education (Grant No. KM200610005016).

Symbols and Abbreviations

CA = water contact angle
 c = gas concentration; for example, $c_{\text{H}_2, \text{permeate}}$ means the H_2 concentration at the permeate side
 d_k = kinetic diameter of gas molecules
 f = gas molar permeance ($\text{mol m}^{-2} \text{s}^{-1} \text{Pa}^{-1}$)
 f^{tot} = overall single gas molar permeance of the supported silica membranes without any corrections
 f^{sup} = single gas molar permeance of the $\gamma\text{-Al}_2\text{O}_3/\alpha\text{-Al}_2\text{O}_3$ supports
 f^{top} = single gas molar permeance of the top silica membranes after correction for the support resistance
 $f^{\text{top-Kn}}$ = single gas molar permeance of the top silica membranes

after correction for the support resistance and the contribution from the defects based on the Knudsen diffusion mechanism
 Δh° = standard partial molar enthalpy of sorption

M = gas molecular weight

u^h = energy barrier for species hopping to an adjacent vacant site in the micropores

u^{tot} = apparent thermal activation energy

α = actual membrane separation factor from a gas mixture measurement

α^* = membrane permselectivity from a single gas measurement

\varnothing_p = pore diameter/width

Q^m = silicon atoms with a chemical environment of $\text{Si}(\text{OSi})_m(\text{OH})_{4-m}$, $m \leq 4$

T^n = silicon atoms with a chemical environment of $\text{RSi}(\text{OSi})_n(\text{OH})_{3-n}$, $n = 1-3$, $R = \text{C}_2\text{H}_4\text{CF}_3$

EtOH = ethanol

TEOS = tetraethyl orthosilicate

TFPTES = (trifluoropropyl)triethoxysilane

TMS = tetramethylsilane

GC = gas chromatography

^{29}Si MAS NMR = ^{29}Si magic angle spinning nuclear magnetic resonance

HK = Horváth–Kawazoe

SF = Saito–Foley

References and Notes

- (1) Nathaniel, L. R.; Juergen, E.; Mohamed, E.; David, T. V.; Jaheon, K.; Michael, O.; Omar, M. Y. *Science* **2003**, *300*, 1127–1129.
- (2) Ritter, J. A.; Ebner, A. D. *Sep. Sci. Technol.* **2007**, *42*, 1123–1193.
- (3) Palo, D. R.; Dagle, R. A.; Holladay, J. D. *Chem. Rev.* **2007**, *107*, 3992–4021.
- (4) Adhikari, S.; Fernando, S. *Ind. Eng. Chem. Res.* **2006**, *45*, 875–881.
- (5) Bredensen, R.; Jordal, K.; Bollard, A. *Chem. Eng. Process.* **2004**, *43*, 1129–1158.
- (6) de Vos, R. M.; Verweij, H. *Science* **1998**, *279*, 1710–1711.
- (7) Duke, M. C.; da Costa, J. C. D.; Lu, G. Q.; Gray, P. G. *AIChE J.* **2006**, *52*, 1729–1735.
- (8) Kanezashi, M.; Asaeda, M. *J. Membr. Sci.* **2006**, *271*, 86–93.
- (9) Kim, Y. S.; Kusakabe, K.; Yang, S. M. *Chem. Mater.* **2003**, *15*, 612–615.
- (10) Ockwig, N. W.; Nenoff, T. M. *Chem. Rev.* **2007**, *107*, 4078–4110.
- (11) de Vos, R. M.; Maier, W. F.; Verweij, H. *J. Membr. Sci.* **1999**, *158*, 277–288.
- (12) Tsai, C. Y.; Tam, S. Y.; Lu, Y. F.; Brinker, C. J. *J. Membr. Sci.* **2000**, *169*, 255–268.
- (13) Giessler, S.; Jordan, L.; da Costa, J. C. D.; Lu, G. Q. *Sep. Purif. Technol.* **2003**, *32*, 255–264.
- (14) Hasegawa, Y.; Kusakabe, K.; Morooka, S. *J. Membr. Sci.* **2001**, *190*, 1–8.
- (15) Lin, Y. S.; Kumakiri, I.; Nair, B. N.; Alsyouri, H. *Sep. Purif. Methods* **2002**, *31*, 229–379.
- (16) Gallaher, G. R.; Liu, P. K. T. *J. Membr. Sci.* **1994**, *92*, 29–44.
- (17) Lebeda, R.; Mendyk, E.; Gierak, A.; Tertykh, V. A. *Colloids Surf., A* **1995**, *105*, 181–189.
- (18) Wei, Q.; Li, J. L.; Song, C. L.; Liu, W.; Chen, C. S. *J. Inorg. Mater.* **2004**, *19*, 417–423.
- (19) Kazakevich, Y. V.; Fadeev, A. Y. *Langmuir* **2002**, *18*, 3117–3122.
- (20) Wagh, P. B.; Ingale, S. V. *Ceram. Int.* **2002**, *28*, 43–50.
- (21) Rao, A. V.; Kulkarni, M. M. *Mater. Chem. Phys.* **2003**, *77*, 819–825.
- (22) El Rassy, H.; Buisson, P.; Bouali, B.; Perrard, A.; Pierre, A. C. *Langmuir* **2003**, *19*, 358–363.
- (23) El Rassy, H.; Pierre, A. C. *J. Non-Cryst. Solids* **2005**, *351*, 1603–1610.
- (24) Camprotrini, R.; Ischia, M.; Armelao, L. *J. Therm. Anal. Calorim.* **2004**, *78*, 657–677.
- (25) Ciriminna, R.; Camprotrini, S.; Pagliaro, M. *Adv. Synth. Catal.* **2004**, *346*, 231–236.
- (26) Delange, R. S. A.; Keizer, K.; Burggraaf, A. J. *J. Porous Mater.* **1995**, *1*, 139–153.
- (27) Horváth, G.; Kawazoe, K. *J. Chem. Eng. Jpn.* **1983**, *16*, 470–475.
- (28) Saito, A.; Foley, H. C. *AIChE J.* **1991**, *37*, 429–436.
- (29) Koros, W. J.; Ma, Y. H.; Shimidzu, T. *Pure Appl. Chem.* **1996**, *68*, 1479–1487.
- (30) Colthup, N. B.; Daly, L. H.; Wiberley, S. E. *Introduction to Infrared and Raman Spectroscopy*; Academic Press: San Diego, 1990.
- (31) Chong, A. S. M.; Zhao, X. S.; Kustedjo, A. T.; Qiao, S. Z. *Microporous Mesoporous Mater.* **2004**, *72*, 33–42.
- (32) Wang, Y. Q.; Yang, C. M.; Zibrowius, B.; Spliethoff, B.; Lindén, M.; Schüth, F. *Chem. Mater.* **2003**, *15*, 5029–5035.
- (33) Wei, Q.; Chen, H. Q.; Nie, Z. R.; Hao, Y. L.; Wang, Y. L.; Li, Q. Y.; Zou, J. X. *Mater. Lett.* **2007**, *61*, 1469–1473.
- (34) Yang, D. J.; Li, J. P.; Xu, Y.; Wu, D.; Sun, Y. H.; Zhu, H. Y.; Deng, F. *Microporous Mesoporous Mater.* **2006**, *95*, 180–186.
- (35) de Vos, R. High-Selectivity, High-Flux Silica Membranes for Gas Separation, Ph.D. Thesis, University of Twente, Enschede, The Netherlands, 1998.
- (36) Verweij, H.; Lin, Y. S.; Dong, J. H. *MRS Bull.* **2006**, *31*, 756–764.
- (37) Nijmeijer, A.; Kruidhof, H.; Bredesen, R.; Verweij, H. *J. Am. Ceram. Soc.* **2001**, *84*, 136–140.
- (38) Wei, Q.; Chen, Z. X.; Wang, Z. H.; Hao, Y. L.; Zou, J. X.; Nie, Z. R. *J. Alloys Compd.* **2005**, *387*, 292–296.
- (39) Duke, M. C.; da Costa, J. C. D.; Do, D. D.; Gray, P. G.; Lu, G. Q. *Adv. Funct. Mater.* **2006**, *16*, 1215–1220.

JP711573F